Microfluidic single-cell measurements of oxidative stress as a function of cell cycle position

Tyler J. Allcroft,[1] Jessica T. Duong,[1] Per Sebastian Skardal,[2] and Michelle L. Kovarik[1,*]

[1] Trinity College, Department of Chemistry, Hartford CT USA
[2] Trinity College, Department of Mathematics, Hartford CT USA
ORCID: 0000-0001-9955-6874
[*] michelle.kovarik@trincoll.edu, ORCID: 0000-0001-8225-2487

Table of Contents Graphic

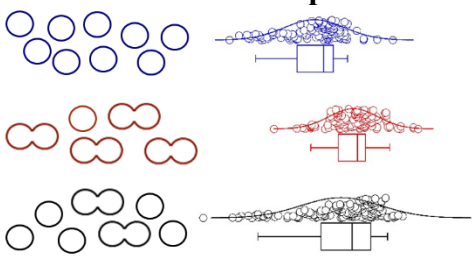

Declarations
The authors have no financial or proprietary interests in any material discussed in this article.
The authors thank Dave Knecht at the University of Connecticut for helpful conversations.
This work was supported by a Cottrell Scholar Award to MLK from Research Corporation for Science Advancement and the National Science Foundation (MCB RUI 2126177).

Abstract

Single-cell measurements routinely demonstrate high levels of variation between cells, but fewer studies provide insight into the analytical and biological sources of this variation. This is particularly true of chemical cytometry, in which individual cells are lysed and their contents separated, compared to more established single-cell measurements of the genome and transcriptome. To characterize population level variation and its sources, we analyzed oxidative stress levels in 1278 individual *Dictyostelium discoideum* cells as a function of exogenous stress level and cell cycle position. Cells were exposed to varying levels of oxidative stress via singlet oxygen generation using the photosensitizer Rose Bengal. Single-cell data reproduced the dose-response observed in ensemble measurements by CE-LIF, superimposed with high levels of heterogeneity. Through experiments and data analysis, we explored possible biological sources of this heterogeneity. No trend was observed between population variation and oxidative stress level, but cell cycle position was a major contributor to heterogeneity in oxidative stress. Cells synchronized to the same stage of cell division were less heterogeneous than unsynchronized cells (RSD of 37-51% vs 93%), and mitotic cells had higher levels of reactive oxygen species than interphase cells. While past research has proposed changes in cell size during the cell cycle as a source of biological noise, the measurements presented here use an internal standard to normalize for effects of cell volume, suggesting that a more complex contribution of cell cycle in heterogeneity of oxidative stress.

Keywords

Microfluidics / Microfabrication, Cell systems / single cell analysis, Bioassays

Introduction

Single-cell measurements are analytical challenging, but necessary to characterize biologically relevant cellular heterogeneity and noise [1, 2]. While some cellular heterogeneity is inevitable due to the stochastic nature of biochemical reactions, this intrinsic noise, along with extrinsic noise due to cell cycle and microenvironment, often plays an important role in the population-level function of genetically identical cells [3]. For example, interaction between two stochastic expression events determines antibody class in individual B cells [4], and stochastic gene expression informs multiple points in differentiation during embryonic development [5]. Most of these investigations probe cellular heterogeneity at the level of the transcriptome or proteome; however, for transient stimuli and acute insults, enzymatic and metabolic responses may occur before changes in gene expression. Thus, direct measurements of enzyme activity, metabolism, and small molecules at the single-cell level are needed to fully understand the physiological role of biological noise, particularly in stress responses.

While cells experience a variety of internal and exogenous stressors, oxidative stress is a ubiquitous source of stress for aerobic organisms. Aerobic cellular respiration is driven by oxidative phosphorylation, and leakage from the electron transport chain is a major source of reactive oxygen species in most cells. Additionally, environmental factors, such as ultraviolet light and chemical exposure, can act as additional sources of reactive oxygen species [6]. Despite reactive oxygen species being a source of stress, cells have evolved to make use of some species in cell signaling and in other functions, including immune response. For example, reactive oxygen species are deployed by macrophages to destroy foreign cells and are hypothesized to play an important role in microbial development [7]. To control reactive oxygen species levels, cells have evolved a variety of antioxidant mechanisms, including enzymes such as catalase and superoxide dismutase and small molecule antioxidants such as ascorbic acid, glutathione, tetrahydrobiopterin, and phenols [6, 8]. Production of these antioxidants requires metabolic input from the cell, and thus, levels may be expected to vary between cells, as has been observed for molecules involved in other stress response pathways [9]. Indeed, previous single-cell studies of reactive oxygen species have found high levels of heterogeneity, especially in stimulated cells exposed to stressors [10–13]. Interestingly, mitochondria have been identified as a major source of extrinsic noise in cells [14–16], suggesting that variation in oxidative stress levels may be an important contributor to non-genetic cellular heterogeneity.

Evaluating the cell-to-cell heterogeneity of reactive oxygen species requires single-cell measurements of oxidative stress in statistically meaningful numbers of cells. Chemical cytometry, in which individual cells are lysed and their contents separated prior to detection, has been used previously to measure many analytes from single cells, including reactive oxygen species indicators [10, 12, 17, 18]. As this technique has matured, it has become possible to measure larger sample sizes. In this work, we present data from 1278 individual *Dictyostelium discoideum* cells. *D. discoideum* is a social amoeba that demonstrates profound non-genetic heterogeneity during its social life cycle and is remarkably resistant to reactive oxygen species [19], making it an interesting model for studies of cellular heterogeneity in oxidative stress response. To eliminate the effects of cell-to-cell variation in size and dye processing and thereby isolate variation in oxidative stress levels, we have used an established method of normalizing the signal for the reactive oxygen species indicator by taking its ratio with the signal for an

internal standard [10, 17, 18]. We then characterized the effects of exogenous reactive oxygen species from singlet oxygen and endogenous reactive oxygen species generated during mitosis on the population distribution of oxidative stress levels. The results address multiple sources of variation in chemical cytometry data, including exogenous stimuli and cell cycle position.

Materials and Methods

Cell culture and synchronization

Dictyostelium discoideum K-AX3 (DBS0236487) was obtained from the Dictyostelium Stock Center and grown in a liquid culture of HL-5 media (14 g/L protease peptone No. 2, 7 g/L Yeast Extract, 1.5 g/L KH_2PO_4, 0.954 g/L Na_2HPO_4•H_2O, pH 6.5) supplemented with 1.35% w/v glucose, 10 μg/mL antimycin, and 30 μg/mL streptomycin [20]. The cells were grown in an incubator shaker at 22 °C and 180 rpm and maintained at a density of 1×10^4 -5×10^6 cells/mL. Cells were synchronized by chilling as described previously [21, 22]. Briefly, cells were resuspended in fresh media at a density of 10^6 cells/mL and incubated with shaking at 9.5 °C for 16 h. The flask was then briefly submerged and swirled in a room temperature water bath to rapidly warm the culture, then incubated with shaking at 22 °C for 1-8 h.

For experiments, cells were resuspended in iron-free low fluorescence media (5 g/L casein peptone, 11 g/L glucose, 0.5 mM NH_4Cl, 0.2 mM $MgCl_2$, 10 μM $CaCl_2$, 13 μM EDTA, 13 μM $ZnSO_4$•H_2O, 18 μM H_3BO_3, 2.6 μM $MnCl_2$•$4H_2O$, 0.7 μM $CoCl_2$•6 H_2O, 0.6 μM CuSO4•$5H_2O$, 81 nM $(NH_4)_6Mo_7O_{24}$•4 H_2O, and 5 mM dibasic potassium phosphate, pH 6.5) [23], plus 5 mM probenecid to inhibit export of the anionic dyes [24]. Cells were loaded with 40 μM Rose Bengal as a photosensitizer, 250 μM carboxyfluorescein diacetate (CFDA) as an internal standard, and 250 μM dihydrodichlorofluorescein diacetate ($DCFH_2DA$) as a reactive oxygen species indicator. After a 20-min, room temperature incubation, the cells were washed once in low fluorescence media with probenecid, and a 200 μL aliquot of cell suspension was transferred to a glass vial, 9.0 cm away from a 4.0 mW/cm^2, 470 nm blue LED light source (ThorLabs) for an exposure time of 0-10 min. After blue light exposure, cells were washed again and resuspended in low fluorescence media with probenecid for analysis.

Ensemble analysis by capillary electrophoresis

For ensemble analysis, 20 million cells were lysed in 80 μL of 90% DMSO, 10% PBS lysis buffer to prevent further oxidation of the $DCFH_2DA$ indicator [25]. Samples were diluted 1:3 in distilled water and stored at 10 °C or lower until analysis. Capillary electrophoresis with 488 nm laser-induced fluorescence detection was performed in an uncoated capillary using a run buffer of 100 mM borate, 100 mM SDS, pH 7.7 and an electric field strength of 400 V/cm on a Beckman Coulter PA-800 Plus.

Microfluidic chemical cytometry

Hybrid PDMS-glass microchannels were prepared using standard soft lithography on SU-8 masters as described previously [26]. Immediately after plasma bonding, each device was filled with small unilamellar vesicles composed of 1 mg/mL egg phosphatidylcholine (Avanti Polar

Lipids) in 10 mM Tris, 150 mM NaCl, pH 7.4 for spontaneous generation of a supported lipid bilayer coating [27]. Microchips were stored at 4 °C for at least 15 minutes and up to 2 weeks and were rinsed for 15 min with low fluorescence media with probenecid prior to use.

For single-cell experiments, cells were resuspended at a density of 5×10^5 cells/mL and added to the cell inlet reservoir of the microchip. The microchip was secured on the stage of an inverted microscope (Olympus IX-73), and platinum wire electrodes connected to a high voltage power supply (LabSmith HVS488LC 3000D) were inserted in the electrophoresis channel inlet and outlet. Fluid content in the cell inlet and waste outlets were adjusted to produce hydrostatic flow at a linear flow rate of ~100 μm/s. The chip position was adjusted to place the focal point of a 40× PlanFluor objective (0.55 NA) 5 mm from the intersection and in alignment with a single point confocal laser-induced fluorescence detection system. The LIF detector consisted of a 488 nm laser (Coherent OBIS LS) operated at 2 mW, a FITC filter, a 500 μm pinhole, a photomultiplier tube (Hamamatsu NO: 34950002), a current-to-voltage converter (Hamamatsu C7319) and a hardware filter (Frequency Devices 900CT/9L8L) set to a corner frequency of 10 Hz. The high voltage power supply and the LIF detection system were controlled through a custom LabVIEW program. A voltage difference of 1000 V was applied across the electrophoresis channel, and the PMT output was collected at a rate of 1000 Hz.

Single-cell electropherograms were analyzed in a custom MATLAB program used in previously published work [28, 29]. When necessary, Cutter 7 software was used to preprocess data to trim electropherograms before peak integration [30]. The datasets generated and analyzed during the current study are available from the corresponding author on reasonable request.

Results and Discussion

Ensemble Measurements

For all experiments, cells were loaded with a reactive oxygen species indicator, $DCFH_2DA$; an internal standard, CFDA; and a photosensitizer, Rose Bengal. After exposure to blue light to produce singlet oxygen, cells were lysed for analysis. While $DCFH_2DA$ is often considered a general reactive oxygen species indicator, it does not react with all species with equal sensitivity. Notably, it has poor sensitivity to superoxide and singlet oxygen [31]. However, singlet oxygen is a potent ROS that rapidly produces other ROS in cells, and many of these species react to produce fluorescent DCF. Ensemble measurements were conducted to identify the appropriate dose of singlet oxygen to induce oxidative stress in the cells without causing cell death. To conduct these experiments, it was necessary to identify a cell lysis buffer that would inhibit the oxidation of residual $DCFH_2$ in cells by oxygen in the air. Based on previous work [25], we used a lysis buffer composed of 90% DMSO, 10% phosphate buffered saline and found stable DCF to CF ratios for repeated runs of the same samples (Fig. 1a inset), even after storage of the lysates at -80 °C for up to one week.

Varying levels of oxidative stress were achieved by varying the exposure time of the cells to blue light. This method is preferred over variation of the concentration of Rose Bengal dye in the cells, which may result in different subcellular localization of the dye [32]. As expected, increasing blue light exposure increased the size of the DCF signal relative to that of the CF

internal standard (Fig. 1). For ensemble lysates of 20 million cells, the peak area of the CF peak showed no trend with blue light exposure time, while the peak area for DCF increased with exposure time (Fig. 1a). The result is a significant effect of blue light exposure time on DCF:CF ratio with $R^2 = 0.889$ for a linear regression. Doses above 10 min of light exposure were not explored because data interpretation is complicated outside the linear range of the dose response curve due to more complex effects from bleaching or changes in localization of the Rose Bengal [32]. Although the R^2 value increased with the addition of the 5 min and 10 min data points, these data appear to fall below the linear trend for 0-2 min, suggesting that these light doses may be approaching or reaching the end of the linear range.

Importantly, cell viability was maintained even at the highest dose of 10 min of light exposure. For the exposure times used here, light doses ranged from 240 to 2400 mJ/cm^2. The upper end of this range has induced ~50% cell death after 6.5 h in cultured neurons [33], and it is below exposures used in bactericidal photodynamic therapy (5 J/cm^2) [34]. Trypan blue staining suggested that *D. discoideum* cell viability ranged from 98% at 0 min light exposure to 94% at 10 min exposure immediately following treatment. Control experiments demonstrated that blue light alone led to some increase in DCF fluorescence in cells that were not loaded with Rose Bengal (Fig. 1b), likely due to the known auto-oxidation of $DCFH_2$ when exposed to light [35, 36]. However, this auto-oxidation was consistently lower than the DCF signal when cells were loaded with Rose Bengal, as generation of singlet oxygen led to additional DCF fluorescence due to production of synchygen species [36].

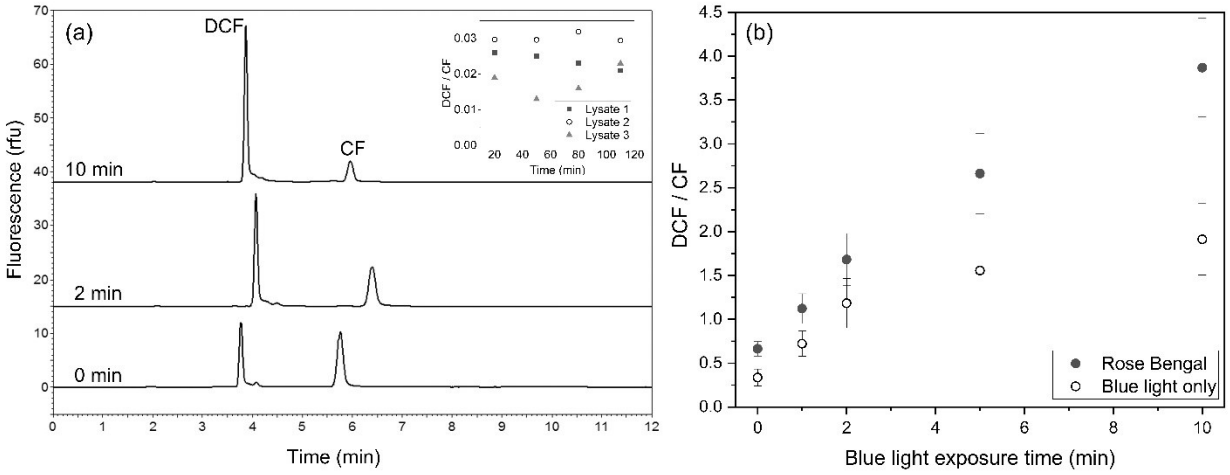

Fig. 1 (a) Representative electropherograms for ensemble lysates of cells loaded with Rose Bengal and lysed after 0, 2, or 10 min of blue light exposure. Inset shows DCF:CF ratio for replicate samples run up to 110 min after cell lysis. (b) DCF:CF ratio for ensemble lysates of cells exposed to varying doses of blue light. Error bars are the standard deviation of six biological replicates on different days.

Single-Cell Measurements

Having identified appropriate levels of oxidative stress, we proceeded to microfluidic experiments to characterize the cell-to-cell variation in oxidative stress for a given dose. As in previous work [17], cells were loaded with the dyes and exposed to stimuli off-chip, moved by

pressure-driven flow to an intersection with the electrophoresis channel, and lysed in the electric field. Cell contents were separated and detected by laser-induced fluorescence 5 mm downstream from the intersection of the cell channel and the electrophoresis channel (Fig. 2a). The migration order of the two dyes was reversed in the microchip separations relative to the capillary separations. This occurred because the microchips are coated with a zwitterionic supported lipid bilayer to reduce cell adhesion [37], resulting in suppressed electroosmotic flow. As a result, the microchip separations were run with reverse polarity, and the more negatively charged CF had higher mobility than the singly charged DCF (Fig. 2a inset).

Individual cells showed substantial variation in both DCF and CF peak signals even for cells exposed to the same duration of blue light exposure (Fig. 2). In some cases, variation in DCF and CF peak areas were correlated, producing low or high peak areas for both dyes (see, e.g., traces (i) and (iii) in Fig. 2a and Fig. 2b). These data demonstrate that although cells exhibited highly variable levels of DCF fluorescence, a large proportion of this variation was due to factors that affected both DCF and the internal standard CF and therefore did not reflect variation in oxidative stress. Variation in cell size, esterase activity, or dye uptake and retention are expected to produce correlated DCF and CF peak areas. In other cases, DCF and CF signals were uncorrelated (trace (iii) in Fig. 2a and Fig. 2b), as when DCF signal – representing oxidative stress – was higher or lower than was typical for the population.

For some treatment groups, data was collected from multiple devices on up to four different days and pooled to obtain data for >100 cells per exposure time. We checked for interday variation using ANOVA and found *p*-values ranging from 0.11 to 0.77 for the five exposure times. While these p-values do not indicate a significant effect of day, they are small enough that further investigation of day-to-day variation may be warranted. Because the microfluidic devices used for single-cell analysis were disposable, they could contribute to interday variation. We checked for variation between microfluidic devices by comparing $n = 53$ cells measured on one device and $n = 52$ cells measured on a second device on the same day using the same batch of cells. We found no significant difference between the two groups ($p = 0.61$) and that variance within each group was much larger than the variance between groups, suggesting that chip-to-chip variation is a small contributor to interday variation. While the internal standard should correct for many other sources of interday variation, other factors remain to be explored, including variation between cell batches. For example, differences in cell density, which may affect metabolic activity and therefore ROS, or in the level of room light exposure during sample preparation may result in different DCF signals from day-to-day. Tighter control of these variables, or high-throughput data collection on a single day, should be considered to minimize effects of day.

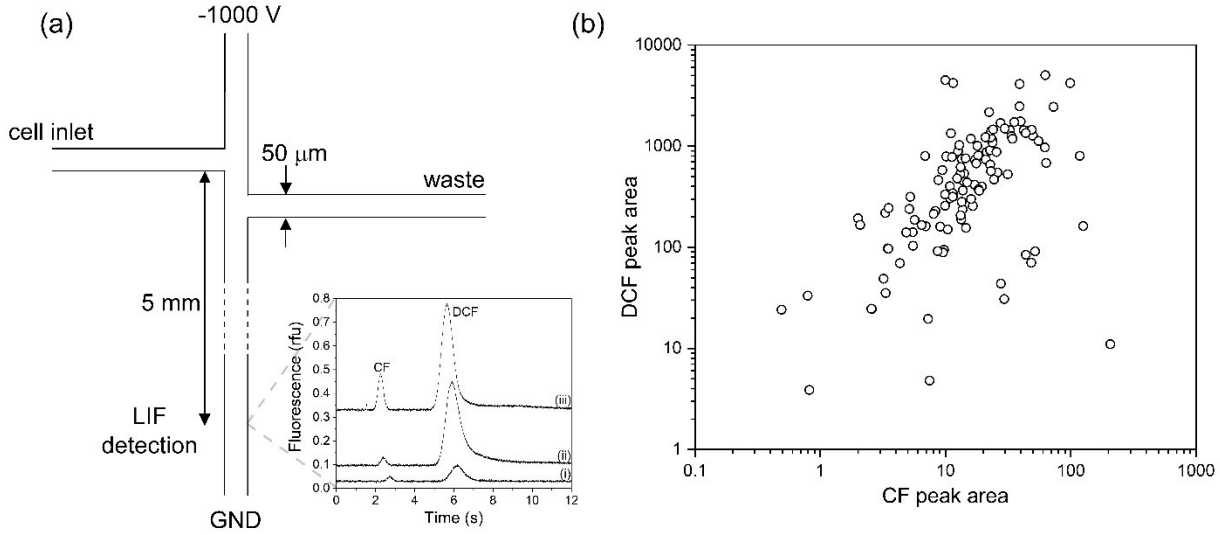

Fig. 2 (a) Microfluidic device used for chemical cytometry in these experiments. (inset) Representative electropherograms for individual cells loaded with Rose Bengal and exposed to blue light for 5 min. (b) Raw peak area data for individual cells loaded with Rose Bengal and exposed to blue light for 5 min. Each point represents a single cell (n = 118).

To extract information about variation in oxidative stress, DCF and CF peak area ratios were calculated (Fig. 3). Compared to the ensemble data (Fig. 1b), DCF:CF ratios were much higher for the single-cell data. This was due to the difference in pH between the electrophoresis buffers used in the capillary and microchip systems. Single-cell separations were conducted in low fluorescence growth medium, maintained at *D. discoideum*'s preferred pH of 6.5, because the microchip design does not permit separate cell and separation buffers. The same buffer could not be used for capillary separations due to its high conductivity. Capillary separations were performed in a lower conductivity buffer at a higher pH of 7.7. While DCF fluorescence was relatively invariant across this pH range, CF fluorescence was significantly decreased at the lower pH due to increased protonation as pH approaches the pK_a of 6.5 (Fig. 3b). This resulted in much higher DCF:CF ratios in the single-cell data relative to the ensemble data; however, the relative change in ratio with blue light dose agreed well between ensemble and single cell data (Fig. S1). DCF:CF ratios were also somewhat higher for cells unexposed to blue light than for comparable control cells in our previous work [17], with a median value of 8 instead of 1.6. This difference could be due to several factors, including differing batches of indicator dye stocks or low-level singlet oxygen production from room light in Rose Bengal loaded cells.

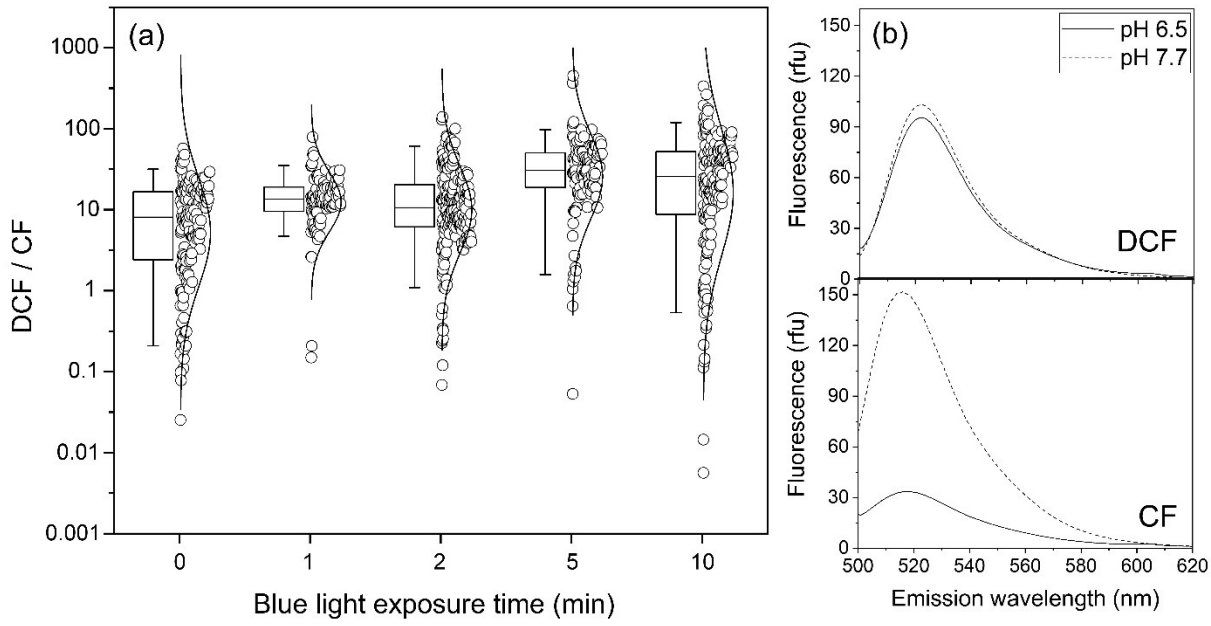

Fig. 3 (a) DCF:CF ratio for single cells exposed to 0 min (n = 162), 1 min (n = 103), 2 min (n = 210), 5 min (n = 118), or 10 min (n = 171) of blue light. Box represents 25th to 75th percentile; whiskers are 5th to 95th percentiles; and line marks the median. Circles show individual cells overlaid with a normal distribution. (b) Fluorescence emission spectra of 100 nM DCF and CF in the microchip (pH 6.5) and capillary electrophoresis (pH 7.7) buffers respectively. Excitation wavelength was 495 nm.

The DCF:CF ratios of individual cells were also noticeably non-normal in distribution. Rather, we found that these data were log-normally distributed and thus present them on a log scale in Fig. 3a. The log distribution was not an artifact of the ratiometric nature of the measurement, as the individual peak areas of the two dyes were also log-normally distributed (Fig. 2b). This population distribution has been observed previously for similar measurements of the nitric oxide indicator DAF-FM-T ratioed to CF [18]. Log-normal distributions occur regularly in nature [38], and a recent publication proposed that first-order kinetics combined with stochasticity could give rise to many naturally occurring log-normal distributions [39]. These experiments use a high loading concentration of $DCFH_2DA$ indicator to prevent saturation of the system [17], thus the reaction may be approximated by first order kinetics with respective to reactive oxygen species. Additionally, a level of stochasticity is expected in single-cell measurements due to intrinsic biological noise [1]. Interestingly, population distributions in our past work using hydrogen peroxide to induce oxidative stress appeared normally distributed [17]. This may have been due to the lower stress levels induced in these cells where lower variance was observed, as log-normal distributions appear less skewed as the variance decreases. However, further exploration is needed of the factors affecting whether log-normality applies to single-cell data and may prove informative in determining the mechanisms of cellular heterogeneity.

Effect of Exogenous Oxidative Stress

As in the ensemble measurements (Fig. 1b), oxidative stress was induced by varying the exposure of Rose Bengal-loaded cells to blue light, and DCF:CF ratio increased with exposure

time. However, this trend in the single-cell data was less obvious due to the log-scale and was superimposed with high levels of cell-to-cell heterogeneity (Fig. 3a). On linearly scaled axes, the magnitude of change in DCF:CF ratio with blue light exposure is comparable for both ensemble and single-cell measurements (Fig. S1). As expected from the ensemble data, blue light exposure had a statistically significant effect on DCF:CF ratio (ANOVA, $p << 0.001$). However, pairwise comparisons of doses did not show a significant difference in DCF:CF ratio for cells exposed to blue light for 1 min exposure compared to 2 min ($p = 0.065$) or 10 min ($p = 0.098$). This observation may be due to the surprisingly narrow distribution of cells for the 1 min dose, combined with the relatively small increase in light exposure from 1 min to 2 min.

In contrast to our previous work [17], we did not observe a clear trend in population variation with oxidative stress level. If cells have underlying heterogeneity in antioxidant levels, one would predict that variance would increase with oxidative stress, as the population distribution widens as cells with low antioxidant levels shift to high DCF:CF ratios, while ratios for cells with high oxidant levels remain relatively unperturbed. While we found that the cells exposed to blue light for 1 min had the lowest variance and cell exposed for 10 min had the highest variance, the unexposed (0 min) population had high variance as well, and no strong trend was observed between light exposure dose and variance. However, while the high end of the DCF:CF ratio distributions moved to higher values as light exposure increased, the low ends of the distributions were less regular, and even at very high blue light exposures, some outlying cells maintained DCF:CF ratios well below the median for unexposed cells. This effect was particularly pronounced for the population of cells exposed to blue light for 10 min (Fig. 3a) and suggests the presence of small numbers of cells within the population with high levels of antioxidants that are more prepared than typical cells to absorb oxidative insults. Even as log-scaled data, the 10 min distribution is poorly fit by a normal distribution due to the long tail to low DCF:CF ratios. Interestingly, past research has shown that moderate variation between cells in the response threshold of a dose response curve can produce broad and tailing distributions at intermediate doses [40]. This effect may explain the more complex relationship between blue light exposure and population variance observed here. However, further study is needed, particularly because the ensemble data for the 10 min light exposure appeared to reach or exceed the end of the linear range (Fig. 1b).

Effect of Cell Cycle

As noted above, we did not observe the specific statistical characteristics of intrinsic biological noise, such as increasing variance with increasing mean values, in these data. However, the data showed a high degree of variability between cells, and past research has shown that extrinsic noise must sometimes be reduced to reveal intrinsic variation [9]. Thus, we turned our attention to sources of extrinsic biological noise, which is linked to identifiable factors, such as cell cycle and microenvironment [1]. To better understand the extrinsic factors that contribute to variance in oxidative stress, we undertook a study of the role of cell cycle, which has been previously identified as a major contributor to biological noise [41, 42]. To do this, we performed single-cell measurements on samples from synchronized cultures.

D. discoideum cell division ceases when cells are chilled to 9.5 °C, and warming the cells to their normal growth temperature of 22 °C induces partially synchronous cell division [21, 43], such

that cell density doubles between 2-5 h after warming (Fig. 4a). We removed cell samples 2 h and 5.5 h after warming the cultures. Cell preparation for the experiment requires ~1 h, so these time points roughly correspond to mitosis and interphase, respectively, although past work has shown that this method does not fully synchronized the culture [43]. Compared to unsynchronized cells, synchronized cells showed similar levels of internal standard CF, but differing levels of DCF (Fig. 4b). Mitotic (2 h) cells showed higher peak areas than average unsynchronized cells, while cells in interphase (5.5 h) showed lower DCF peak areas. As a result, DCF:CF ratios were higher for mitotic cells than for cells in interphase (Fig. 4c). This observation matches with past research showing that cells experience higher levels of oxidative stress, as measured by DCF fluorescence, during cell division [44, 45]. Additionally, cell division machinery has been shown to regulate both oxidative phosphorylation and mitochondrial biogenesis [46].

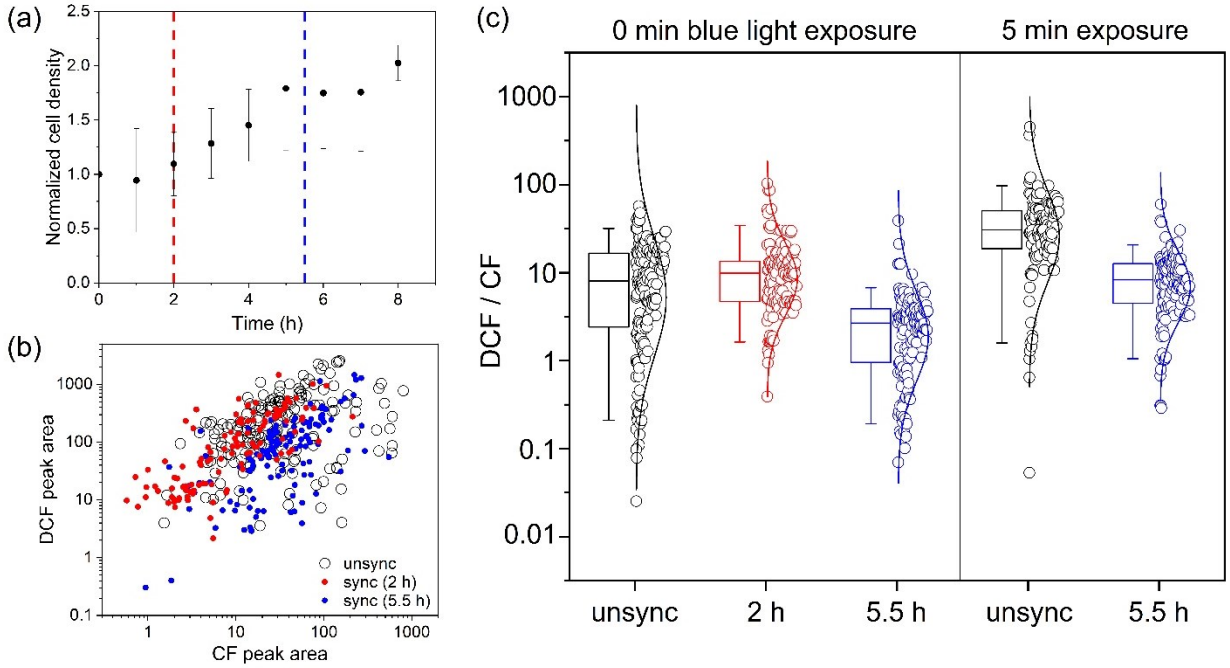

Fig. 4 (a) Normalized cell densities as a function of time after warming chilled cells up to growth temperature. Error bars are the standard deviations of three biological replicates. (b) Raw peak area data for individual cells loaded with Rose Bengal and exposed to blue light for 0 min for both unsynchronized cells and synchronized cells 2 h (red) and 5.5 h (blue) after warming. Each point represents a single cell (n = 162 for unsynchronized cells, 123 cells for 2 h and 130 for 5.5 h). (c) DCF: CF ratio for unsynchronized cells and synchronized cells 2 h or 5.5 h after warming exposed to 0 min or 5 min of blue light. Box represents 25th to 75th percentile; whiskers are 5th to 95th percentiles; and line marks the median. Circles show individual cells overlaid with a normal distribution. Data for unsynchronized cells are repeated from Fig. 3 for comparison (n = 162 for 0 min and 118 for 5 min). Data for synchronized cells includes n = 123, 130, and 131, respectively for 2 h, 0 min; 5.5 h, 0 min; and 5.5h, 5 min.

The distributions of DCF:CF ratios for the synchronized cells overlapped with distribution for unsynchronized cells but were significantly narrower (F-test p-values < 10^{-3}). The relative

standard deviations of the log (DCF/CF) values were 37% and 51% for the 2 h and 5.5 h synchronized samples, respectively, compared to 91% for the unsynchronized cells. The narrowing of these distributions suggests that cell cycle is a significant contributor to extrinsic biological noise in oxidative stress. Some past research on the role of cell cycle in biological noise has attributed variation to the effects of cell volume [47, 48]; however, the data presented here should minimize the effect of cell volume since larger cells will uptake proportionately more CF internal standard. Interestingly, like cell cycle position, mitochondria have also been identified as a major contributor to non-genetic heterogeneity in the form of extrinsic biological noise [14–16]. Preliminary experiments in our lab using Rhodamine 123 to stain cells for mitochondrial membrane potential suggest that mitochondrial activity is higher in the 2 h cell samples than in the 5.5 h cell samples (data not shown). Thus, while the data in Fig. 4c demonstrate that cell cycle position is a key contributor to biological noise in oxidative stress response, its effect may be mediated by mitochondrial activity.

We also investigated whether the population distributions for the cells sampled at 2 h and 5.5 h were unimodal. *D. discoideum* lacks a G1 stage, so its cell cycle consists of mitosis (M), synthesis (S), and the G2 stage of cell growth. The G2 phase comprises 6.5-7 h of the 8 h cell cycle when cells are grown in axenic media [49]. Consequently, we expected that synchronized cells sampled at 5.5 h would be exclusively G2 cells. In contrast, mitosis occurs in under 30 min in *D. discoideum*, and cell staining and data collection in these experiments lasted more than 1 h. Additionally, a previous study using the same synchronization method found that gene expression for S phase and DNA synthesis began immediately after warming, but DNA synthesis peaked 3 h later and genes expressed exclusively at the M/G2 transition were enriched less than three-fold, suggesting incomplete synchronization [43]. Despite this limitation, we chose to use this method to avoid metabolic artifacts of chemical methods of cell cycle synchronization, which may affect reactive oxygen species levels in cells [50]. Thus, while the 2 h synchronized cell samples were enriched in mitotic cells, they are expected to also contain cells at other stages of the cell cycle. Replotting the data from Fig. 4c as histograms suggested that the distribution for the 2 h cells, in contrast to the unsynchronized or 5.5 h cells, may be multimodal (Fig. S2). We performed Hartigan's dip test for unimodality [51] for all three samples. The unsynchronized and 5.5 h data were clearly unimodal ($p = 0.990$ for each), but the result was inconclusive for the 2 h sample ($p = 0.233$). We also estimated the number of mitotic cells in the unsynchronized population using the data for the 2 h and 5.5 h cells (Supplemental Information), but these results suggested that >40% of cells were mitotic, showing poor agreement with past work on the relative duration of these stages. This discrepancy suggests that sampling at 2 h and 5.5 h after warming the cells did not fully capture the range of oxidative stress levels present in the unsynchronized samples. Past research has shown that ROS levels increase steadily during the cell cycle, rather than changing sharply with stage [44]. Our 5.5 h sample sampled cells early in G2 (Fig. 4a) and therefore likely underestimates the ROS level in all interphase cells and thus their contribution to the unsynchronized population.

Characterization and control of oxidative stress in cells at various cell cycle points is important to elucidate the role of reactive oxygen species in cell division. Past research has shown that oxidation of biomolecules increases during mitosis, and antioxidant treatment can arrest the cell cycle, leading to the hypothesis that biomolecule oxidation acts as an internal cellular marker of progress through mitosis [44, 45]. The ability to control the redox state of the cell independent of

cell cycle may be of interest in further exploring this hypothesis. In addition to studying unstressed, synchronized cells, we also exposed a population of synchronized interphase cells to blue light to induce higher levels of oxidative stress. As in the unstressed populations, the interphase cells exposed to blue light showed lower oxidative stress and less heterogeneity than unsynchronized cells treated with the same blue light exposure (Fig. 4c). In the interphase cells, a 5 min exposure to blue light induced oxidative stress comparable to that of untreated 2 h samples ($p = 0.083$), providing a preliminary estimate of the relative scale of exogenous stimulus needed to mimic endogenous oxidative stress during mitosis.

Conclusions

Chemical cytometry experiments have helped to establish that the contents of cells are highly heterogeneous, but this technique has been applied less frequently to investigate the sources of that heterogeneity. This work demonstrates how targeted single-cell analysis of oxidative stress can generate information about population distributions that inform biological hypotheses about non-genetic heterogeneity. Future work should focus on deeper mathematical characterization of these population distributions and on mapping them onto molecular mechanisms of heterogeneity. Additionally, further investigation into the magnitude and sources of non-biological variation is needed, including characterizing levels of instrumental noise using standards that account for variation in lysis and further evaluation of interday variation. Even as throughput improves, interday variation will remain important for longitudinal studies of how population distributions change over the course of long-term stimuli rather than acute stress.

Acknowledgments

The authors thank Dave Knecht at the University of Connecticut for helpful conversations. This work was supported by a Cottrell Scholar Award to MLK from Research Corporation for Science Advancement and the National Science Foundation (MCB RUI 2126177).

Conflict of Interest

The authors declare that they have no conflicts of interest.

References

1. Arriaga EA (2009) Determining biological noise via single cell analysis. Anal Bioanal Chem 393:73–80. https://doi.org/10.1007/s00216-008-2431-z

2. Altschuler SJ, Wu LF (2010) Cellular Heterogeneity: Do Differences Make a Difference? Cell 141:559–563. https://doi.org/10.1016/j.cell.2010.04.033

3. Samoilov MS, Price G, Arkin AP (2006) From fluctuations to phenotypes: the physiology of noise. Sci STKE 2006:re17. https://doi.org/10.1126/stke.3662006re17

4. Horton MB, Cheon H, Duffy KR, Brown D, Naik SH, Alvarado C, Groom JR, Heinzel S, Hodgkin PD (2022) Lineage tracing reveals B cell antibody class switching is stochastic,

cell-autonomous, and tuneable. Immunity 55:1843-1855.e6. https://doi.org/10.1016/j.immuni.2022.08.004

5. Chubb JR (2017) Symmetry breaking in development and stochastic gene expression. Wiley Interdiscip Rev Dev Biol 6:. https://doi.org/10.1002/wdev.284

6. Krumova K, Cosa G (2016) Chapter 1 Overview of Reactive Oxygen Species. 1:1–21. https://doi.org/10.1039/9781782622208-00001

7. Aguirre J, Ríos-Momberg M, Hewitt D, Hansberg W (2005) Reactive oxygen species and development in microbial eukaryotes. Trends Microbiol 13:111–118. https://doi.org/10.1016/j.tim.2005.01.007

8. Park S-O, Kim H-L, Lee S-W, Park YS (2013) Tetrahydropteridines possess antioxidant roles to guard against glucose-induced oxidative stress in Dictyostelium discoideum. BMB Rep 46:86–91. https://doi.org/10.5483/BMBRep.2013.46.2.128

9. Newman JRS, Ghaemmaghami S, Ihmels J, Breslow DK, Noble M, DeRisi JL, Weissman JS (2006) Single-cell proteomic analysis of S. cerevisiae reveals the architecture of biological noise. Nature 441:840–846. https://doi.org/10.1038/nature04785

10. Metto EC, Evans K, Barney P, Culbertson AH, Gunasekara DB, Caruso G, Hulvey MK, Fracassi da Silva JA, Lunte SM, Culbertson CT (2013) An integrated microfluidic device for monitoring changes in nitric oxide production in single T-lymphocyte (Jurkat) cells. Analytical Chemistry 85:10188–10195. https://doi.org/10.1021/ac401665u

11. Zhang L, Vertes A (2015) Energy Charge, Redox State, and Metabolite Turnover in Single Human Hepatocytes Revealed by Capillary Microsampling Mass Spectrometry. Anal Chem 87:10397–10405. https://doi.org/10.1021/acs.analchem.5b02502

12. Li Q, Chen P, Fan Y, Wang X, Xu K, Li L, Tang B (2016) Multicolor fluorescence detection-based microfluidic device for single-cell metabolomics: Simultaneous quantitation of multiple small molecules in primary liver cells. Analytical Chemistry 88:8610–8616. https://doi.org/10.1021/acs.analchem.6b01775

13. Liu F, Whitley J, Ng NL, Lu H (2020) Time-Resolved Single-Cell Assay for Measuring Intracellular Reactive Oxygen Species upon Exposure to Ambient Particulate Matter. Environ Sci Technol 54:13121–13130. https://doi.org/10.1021/acs.est.0c02889

14. Johnston IG, Gaal B, Neves RP das, Enver T, Iborra FJ, Jones NS (2012) Mitochondrial Variability as a Source of Extrinsic Cellular Noise. PLOS Computational Biology 8:e1002416. https://doi.org/10.1371/journal.pcbi.1002416

15. Guantes R, Díaz-Colunga J, Iborra FJ (2015) Mitochondria and the non-genetic origins of cell-to-cell variability: More is different. BioEssays 38:64–76. https://doi.org/10.1002/bies.201500082

16. Dhar R, Missarova AM, Lehner B, Carey LB (2019) Single cell functional genomics reveals the importance of mitochondria in cell-to-cell phenotypic variation. eLife 8:e38904. https://doi.org/10.7554/elife.38904

17. Rodogiannis K, Duong JT, Kovarik ML (2018) Microfluidic single-cell analysis of oxidative stress in Dictyostelium discoideum. Analyst 143:3643–3650. https://doi.org/10.1039/C8AN00752G

18. Sibbitts J, Culbertson CT (2020) Measuring stimulation and inhibition of intracellular nitric oxide production in SIM-A9 microglia using microfluidic single-cell analysis. Anal Methods 12:4665–4673. https://doi.org/10.1039/D0AY01578D

19. Katoch B, Begum R (2003) Biochemical basis of the high resistance to oxidative stress in Dictyostelium discoideum. J Biosci 28:581–588

20. Fey P, Dodson RJ, Basu S, Chisholm RL (2013) One Stop Shop for Everything Dictyostelium: dictyBase and the Dicty Stock Center in 2012. In: Eichinger L, Rivero F (eds) Dictyostelium discoideum Protocols. Humana Press, Totowa, NJ, pp 59–92

21. Maeda Y (1986) A New Method for Inducing Synchronous Growth of Dictyostelium discoideum Cells Using Temperature Shifts. Microbiology 132:1189–1196. https://doi.org/10.1099/00221287-132-5-1189

22. Araki T, Nakao H, Takeuchi I, Maeda Y (1994) Cell-Cycle-Dependent Sorting in the Development of Dictyostelium Cells. Developmental Biology 162:221–228. https://doi.org/10.1006/dbio.1994.1080

23. MacWilliams H Low Fluorescence Axenic Medium. In: Low fluorescence axenic medium. http://dictybase.org/techniques/media/lowflo_medium.html. Accessed 5 Jun 2017

24. Steinberg TH, Newman AS, Swanson JA, Silverstein SC (1987) Macrophages possess probenecid-inhibitable organic anion transporters that remove fluorescent dyes from the cytoplasmic matrix. J Cell Biol 105:2695–2702

25. Wang G, Gong Y, Burczynski FJ, Hasinoff BB (2008) Cell lysis with dimethyl sulphoxide produces stable homogeneous solutions in the dichlorofluorescein oxidative stress assay. Free Radical Research 42:435–441. https://doi.org/10.1080/10715760802074462

26. McDonald JC, Duffy DC, Anderson JR, Chiu DT, Wu H, Schueller OJ, Whitesides GM (2000) Fabrication of microfluidic systems in poly(dimethylsiloxane). Electrophoresis 21:27–40

27. Phillips KS, Kottegoda S, Kang KM, Sims CE, Allbritton NL (2008) Separations in poly(dimethylsiloxane) microchips coated with supported bilayer membranes. Anal Chem 80:9756–9762. https://doi.org/10.1021/ac801850z

28. Kovarik ML, Shah PK, Armistead PM, Allbritton NL (2013) Microfluidic chemical cytometry of peptide degradation in single drug-treated acute myeloid leukemia cells. Anal Chem 85:4991–4997. https://doi.org/10.1021/ac4002029

29. Kovarik ML, Dickinson AJ, Roy P, Poonnen RA, Fine JP, Allbritton NL (2014) Response of single leukemic cells to peptidase inhibitor therapy across time and dose using a microfluidic device. Integr Biol 6:164–174. https://doi.org/10.1039/C3IB40249E

30. Shackman JG, Watson CJ, Kennedy RT (2004) High-throughput automated post-processing of separation data. J Chromatogr A 1040:273–282

31. Halliwell B, Whiteman M (2004) Measuring reactive species and oxidative damage in vivo and in cell culture: how should you do it and what do the results mean? Br J Pharmacol 142:231–255. https://doi.org/10.1038/sj.bjp.0705776

32. Kochevar IE, Redmond RW (2000) Photosensitized production of singlet oxygen. Methods Enzymol 319:20–28. https://doi.org/10.1016/s0076-6879(00)19004-4

33. Valencia A, Morán J (2004) Reactive oxygen species induce different cell death mechanisms in cultured neurons. Free Radical Biology and Medicine 36:1112–1125. https://doi.org/10.1016/j.freeradbiomed.2004.02.013

34. Uekubo A, Hiratsuka K, Aoki A, Takeuchi Y, Abiko Y, Izumi Y (2016) Effect of antimicrobial photodynamic therapy using rose bengal and blue light-emitting diode on Porphyromonas gingivalis in vitro: Influence of oxygen during treatment. Laser Ther 25:299–308. https://doi.org/10.5978/islsm.16-OR-25

35. Reiniers MJ, van Golen RF, Bonnet S, Broekgaarden M, van Gulik TM, Egmond MR, Heger M (2017) Preparation and Practical Applications of 2′,7′-Dichlorodihydrofluorescein in Redox Assays. Anal Chem 89:3853–3857. https://doi.org/10.1021/acs.analchem.7b00043

36. Bilski P, Belanger AG, Chignell CF (2002) Photosensitized oxidation of 2′,7′-dichlorofluorescin: singlet oxygen does not contribute to the formation of fluorescent oxidation product 2′,7′-dichlorofluorescein. Free Radical Biology and Medicine 33:938–946. https://doi.org/10.1016/S0891-5849(02)00982-6

37. Clapis JR, Fan MJ, Kovarik ML (2021) Supported bilayer membranes for reducing cell adhesion in microfluidic devices. Anal Methods 13:1535–1540. https://doi.org/10.1039/d0ay01992e

38. Limpert E, Stahel WA, Abbt M (2001) Log-normal Distributions across the Sciences: Keys and Clues: On the charms of statistics, and how mechanical models resembling gambling machines offer a link to a handy way to characterize log-normal distributions, which can provide deeper insight into variability and probability—normal or log-normal: That is the question. BioScience 51:341–352. https://doi.org/10.1641/0006-3568(2001)051[0341:LNDATS]2.0.CO;2

39. Andersson A (2021) Mechanisms for log normal concentration distributions in the environment. Sci Rep 11:16418. https://doi.org/10.1038/s41598-021-96010-6

40. Dobrzyński M, Nguyen LK, Birtwistle MR, von Kriegsheim A, Blanco Fernández A, Cheong A, Kolch W, Kholodenko BN (2014) Nonlinear signalling networks and cell-to-cell variability transform external signals into broadly distributed or bimodal responses. J R Soc Interface 11:20140383. https://doi.org/10.1098/rsif.2014.0383

41. Barron M, Li J (2016) Identifying and removing the cell-cycle effect from single-cell RNA-Sequencing data. Sci Rep 6:33892. https://doi.org/10.1038/srep33892

42. Keren L, Dijk D van, Weingarten-Gabbay S, Davidi D, Jona G, Weinberger A, Milo R, Segal E (2015) Noise in gene expression is coupled to growth rate. Genome Res 25:1893–1902. https://doi.org/10.1101/gr.191635.115

43. Strasser K, Bloomfield G, MacWilliams A, Ceccarelli A, MacWilliams H, Tsang A (2012) A Retinoblastoma Orthologue Is a Major Regulator of S-Phase, Mitotic, and Developmental Gene Expression in Dictyostelium. PLOS ONE 7:e39914. https://doi.org/10.1371/journal.pone.0039914

44. Havens CG, Ho A, Yoshioka N, Dowdy SF (2006) Regulation of Late G1/S Phase Transition and APCCdh1 by Reactive Oxygen Species. Mol Cell Biol 26:4701–4711. https://doi.org/10.1128/MCB.00303-06

45. Patterson JC, Joughin BA, van de Kooij B, Lim DC, Lauffenburger DA, Yaffe MB (2019) ROS and Oxidative Stress are Elevated in Mitosis During Asynchronous Cell Cycle Progression and are Exacerbated by Mitotic Arrest. Cell Syst 8:163-167.e2. https://doi.org/10.1016/j.cels.2019.01.005

46. Salazar-Roa M, Malumbres M (2017) Fueling the Cell Division Cycle. Trends Cell Biol 27:69–81. https://doi.org/10.1016/j.tcb.2016.08.009

47. Halter M, Elliott JT, Hubbard JB, Tona A, Plant AL (2009) Cell volume distributions reveal cell growth rates and division times. Journal of Theoretical Biology 257:124–130. https://doi.org/10.1016/j.jtbi.2008.10.031

48. Thomas P, Shahrezaei V (2021) Coordination of gene expression noise with cell size: analytical results for agent-based models of growing cell populations. Journal of The Royal Society Interface 18:20210274. https://doi.org/10.1098/rsif.2021.0274

49. Weeks G, Weijer CJ (1994) The Dictyostelium cell cycle and its relationship to differentiation. FEMS Microbiology Letters 124:123–130. https://doi.org/10.1111/j.1574-6968.1994.tb07274.x

50. Ligasová A, Koberna K (2021) Strengths and Weaknesses of Cell Synchronization Protocols Based on Inhibition of DNA Synthesis. International Journal of Molecular Sciences 22:10759. https://doi.org/10.3390/ijms221910759

51. Hartigan JA, Hartigan PM (1985) The Dip Test of Unimodality. The Annals of Statistics 13:70–84. https://doi.org/10.1214/aos/1176346577